Chemical Geology 281 (2011) 93–102

Contents lists available at ScienceDirect

Chemical Geology

journal homepage: www.elsevier.com/locate/chemgeo

Research paper

Zircon U–Pb geochronology from the Paraná bimodal volcanic province support a brief eruptive cycle at ~135 Ma

Viter Magalhães Pinto [a], Léo Afraneo Hartmann [b,*], João Orestes S. Santos [c], Neal Jesse McNaughton [d], Wilson Wildner [e]

[a] Departamento de Geologia, Instituto de Geociências, Universidade Federal de Roraima, Avenida Cap. Ene Garcez, Boa Vista, Roraima, Brazil
[b] Instituto de Geociências, Universidade Federal do Rio Grande do Sul, Av. Bento Gonçalves 9500, 91500-970 Porto Alegre, Rio Grande do Sul, Brazil
[c] Centre for Exploration Targeting, University of Western Australia, 35 Stirling Highway, Crawley, 6009 Perth, WA, Australia
[d] John de Laeter Centre, Curtin University of Technology, Bentley, 6845 Perth, WA, Australia
[e] Companhia de Pesquisa de Recursos Minerais, Rua Banco da Província, 105, 90840-030 Porto Alegre, Rio Grande do Sul, Brazil

ARTICLE INFO

Article history:
Received 8 January 2010
Received in revised form 4 November 2010
Accepted 30 November 2010
Available online 8 December 2010

Editor: B. Bourdon

Keywords:
Paraná magmatic province
Zircon
SHRIMP geochronology
Basalt
Rhyodacite

ABSTRACT

Ion microprobe U–Pb isotopic data on zircons from the Paraná magmatic province are presented from one tholeiitic (high-Ti Pitanga type) and three felsic volcanic rocks from the low-Ti Palmas and high-Ti Chapecó types. Igneous zircons from the four volcanic rocks yield volcanism ages within error: i.e. 134.4 ± 1.1 Ma (basalt), 134.6 ± 1.4 Ma (rhyodacite), 134.8 ± 1.4 (quartz latite) and 135.6 ± 1.8 Ma (quartz latite). The age of Paraná magmatism based on previous Ar–Ar geochronology has two divergent ranges: 1) 1 to 2 million years with magmatic peak at 131–133 Ma, and 2) over ~10 m.y. between 137 and 127 Ma. Our results show that the bimodal volcanics of the province, at least to the south of the Piquiri lineament, have very high effusion rates over a brief period with a main pulse at ~135 Ma, about 2% older than proposal 1, more akin to a short period of magmatism. These results are most significant for the understanding of time relations in this large intraplate magmatic province.

1. Introduction

Geochronology has played a critical role in constraining the time scale of magmatism in the Paraná province, and some of the relations between magmatism, stratigraphy, mantle geodynamics, and tectonic processes such as continental fragmentation. The Paraná magmatic province has been the subject of several K–Ar and Ar–Ar and a few Rb–Sr and U–Pb geochronological studies. Over 200 K–Ar whole-rock and feldspar analyses (reviewed by Campos et al., 1988) show a wide range of ages (~150 to 110 Ma) indicating problems with both excess argon and post-crystallization argon loss. Mantovani et al. (1985) reported a combined Rb–Sr mineral isochron of 135 ± 3.5 Ma from three Chapecó rhyolite samples. Nevertheless, whole-rock data from 13 samples of Palmas-type rhyolites showed excess scatter on an isochron diagram, probably due to some combination of heterogeneous initial $^{87}Sr/^{86}Sr$ and secondary mobility of Rb and Sr (Cordani et al., 1980; Renne, 1997).

In the 1990s, the dating efforts concentrated on the potential of the $^{40}Ar/^{39}Ar$ technique to obtain more precise Paraná volcanic age estimates (Baksi et al., 1991; Renne et al., 1992, 1996a,b; Turner et al., 1994; Stewart et al., 1996; Ernesto et al., 1999; Mincato et al., 2000). These Ar–Ar radiometric studies report divergent age ranges and interpretations. For instance, Turner et al. (1994) and Stewart et al. (1996) report a wide age range for the Paraná volcanism over 10 m.y. between ~137 and 127 Ma. They also mention that Ar–Ar analyses indicate that magmatism within the Paraná magmatic province migrated from northwest to southeast. On the other hand, Renne et al. (1992, 1996a,b) published detailed $^{40}Ar/^{39}Ar$ studies that indicate a main magmatic emplacement of preserved volcanic rocks in a brief period of time (1–3 m.y.) and a peak at 133–131 Ma. This short interval is comparable to other flood volcanic sequences, such as the Siberian and Deccan provinces (Renne et al., 1996a). A major question in flood basalt provinces has been over the duration of the main volumetric pulse of the magmatism. Therefore, in addition to reliable geochronology, it is also critical to understand the volcanic stratigraphy of the province. For example, the initial study of Renne et al. (1992) argued for a short duration of magmatism in the Paraná, but this was based on a single road section in the south of the province and ignored stratigraphic evidence that a significant part of the lava pile further north was not represented in the study.

Based on $^{40}Ar/^{39}Ar$ dating and paleomagnetic data, Ernesto et al. (1999) reported that the northern Paraná magmatic province (north

* Corresponding author. Tel.: +55 51 33087202.
E-mail address: leo.hartmann@ufrgs.br (L.A. Hartmann).

0009-2541 © 2010 Elsevier B.V. Open access under the Elsevier OA license.
doi:10.1016/j.chemgeo.2010.11.031

of the Rio Piquiri lineament, Fig. 1a) is younger than the southern Paraná magmatic province or the adjacent Etendeka province in Namibia, resulting in a northward migration of volcanism, consistent with the regional lava stratigraphy as inferred by Peate et al. (1990). The youngest volcanic events detected show that the eruption of lavas stopped at 131.4 ± 0.5 to 129.2 ± 0.4 Ma (Renne et al., 1996a,b); these ages are from a related NW-trending Ponta Grossa dyke swarm that are compositionally similar to the Paraná and Paranapanema basaltic magma types. Deckart et al. (1998) also found similar young N-trending dykes in Santa Catarina and NE-trending dykes in the São Paulo–Rio de Janeiro region.

Geochronological studies using the Ar–Ar technique have been undertaken on the Etendeka magmatism on the conjugate margin in Namibia, Africa. There are good direct stratigraphic and compositional correlations between the Khumib and Tafelberg basalt types of the Etendeka, with, respectively, the Urubici and Gramado types of the Paraná (Peate, 1997; Marsh et al., 2001). Eruptive ages of 127–132 Ma are reported for the Etendeka (Milner et al., 1995; Renne et al., 1996b) and are compared with equivalent lavas from southern Uruguay (Kirstein et al., 2001).

Zircon U–Pb ages were reported more recently from intrusive and extrusive rocks. Lustrino et al. (2005) obtained a Concordia age of 128.1 ± 1.8 Ma in a conventional U–Pb isotopic study of two populations of zircon from the Valle Chico quartz-syenite (SE Uruguay), considered linked with the formation of the Paraná–Etendeka Igneous Province. Wildner et al. (2006) analyzed zircons from felsic volcanic rocks of Chapecó type and obtained ages of ~135 Ma: these data were incorporated in this work in order to compare with new data.

We present new U–Pb sensitive high-resolution ion microprobe (SHRIMP II) data on igneous zircons from volcanic rocks in the province. The selected rocks cover the bimodal compositional spectrum from basalt to quartz latite and rhyodacite, and include rocks from the basaltic high-Ti Pitanga chemical type, the felsic low-Ti Palmas type, and felsic high-Ti Chapecó type. The geochemistry of the dated samples yields the correct classification and comparison with published data in the context of Paraná volcanic magmatism. This

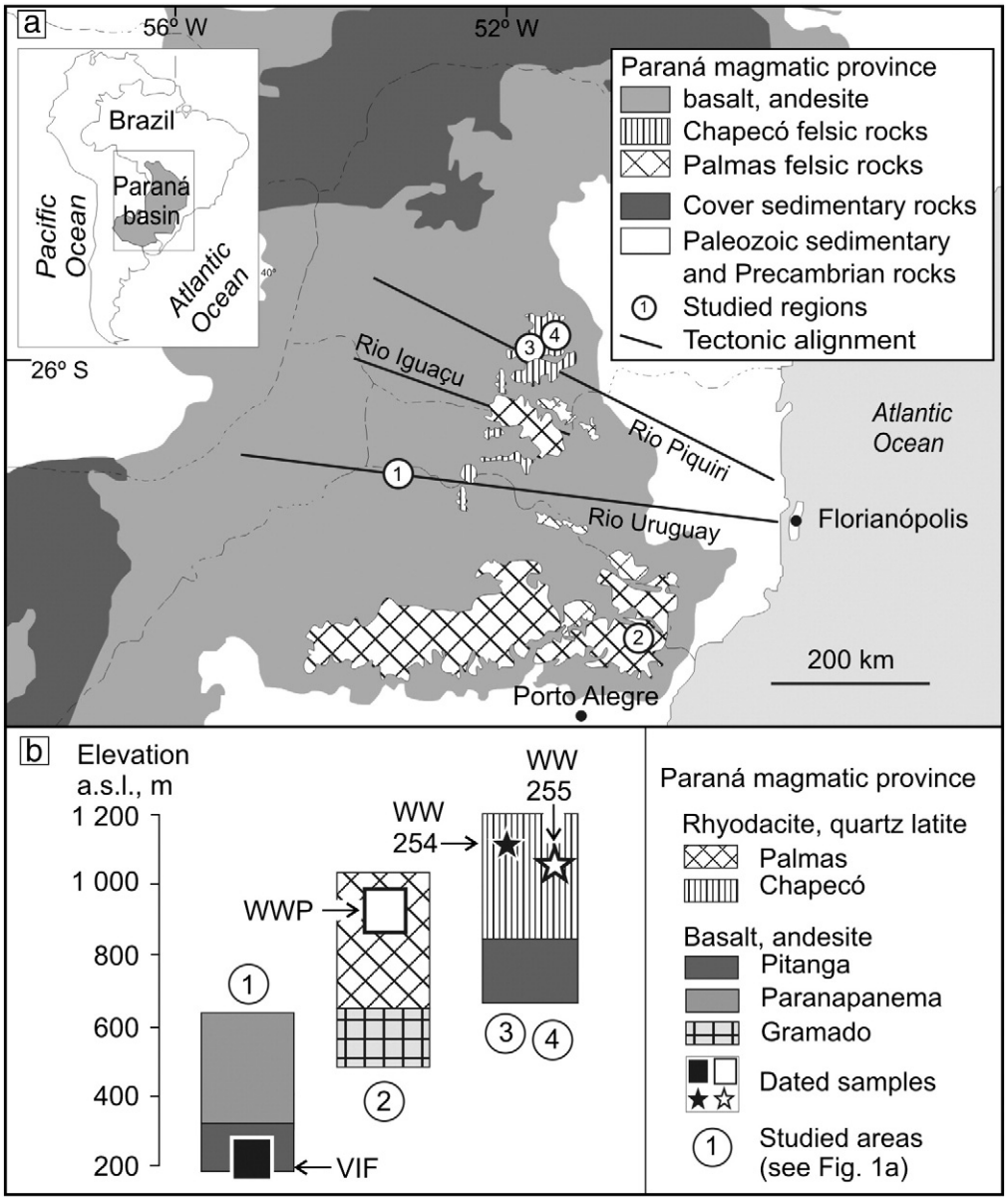

Fig. 1. a) Simplified geological map of the Paraná magmatic province centered in southeastern Brazil (modified from Peate et al., 1992 and Nardy et al., 2008), showing the location of studied areas and of dated samples (white label). b) Stratigraphic column of studied areas with dated samples. Regional location is indicated in Fig. 1a.

study is therefore directed to a better understanding of the time relations in both basic and acid magma generation in one of the largest intracontinental magmatic provinces in the world.

1.1. Geological background

The Paraná magmatic province in South America and the minor Etendeka remnant in Namibia, Africa, consist of basalts and rhyolites with a volume in excess of 800,000 km^3 (Peate and Hawkesworth, 1996), and are one of the largest igneous provinces (LIPs) in the world, closely related with the Lower Cretaceous opening of the South Atlantic Ocean (Peate et al., 1992). The large volume of magma generated in a comparatively short period of time has long been linked to upwelling of deep and hot mantle plumes, now reflected by the Tristan mantle plume (Morgan, 1971; Richards et al., 1989; White and McKenzie, 1989; Gibson et al., 1995; Self et al., 1997). This plume decompression model (White and McKenzie, 1989, 1995) predicts that the LIP reflects mainly a deep asthenospheric mantle origin (e.g. Deccan). However, the isotopic and geochemical features of some LIPs, notably in the Mesozoic Gondwana flood basalts, such as the Paraná, show evidence that their origin is related to a lithospheric heterogeneous mantle source and suggest that for Paraná magmatism an asthenospheric plume origin is compatible only as a thermal perturbation which triggered the melting process of the lithospheric mantle (e.g. Turner et al., 1994; Turner and Hawkesworth, 1995; Peate and Hawkesworth, 1996; Comin-Chiaramonti et al., 1997; Marques et al., 1999). On the other hand, Coltice et al. (2007) suggest that the generation of huge volumes of lava in the Mesozoic LIPs (Karoo, Paraná and Ferrar) was a consequence of heating of the mantle underneath supercontinent Gondwana, and the presence of a plume was not required.

The Paraná magmatic province covers an area of at least 1.2×10^6 km^2 in southeastern South America (Fig. 1a) and comprises the Serra Geral Formation, the formal stratigraphic name for the Paraná lavas in Brazil. The Paraná lavas have bimodal compositions of basalt and rhyodacite. Overall, the formation is composed mostly of tholeiitic basalt and basaltic andesite (>90% by volume), but near the continental margin significant quantities of felsic rocks cap the sequence (recent review in Hartmann et al., 2010). These felsic successions cover ~2.5% of the total volume of volcanic rocks in the Paraná magmatic province (Nardy et al., 2001). Felsic rocks are found at depths over 400 m in the depocenter because the felsic successions dip to the center of the Paraná basin. The thickness of the volcanic sequence reaches 1700 m near the depocenter.

On the basis of the geochemical similarities, Peate et al. (1992) proposed a division of the basaltic rocks into two major types, subdivided into six distinct tholeiitic magma types: 1) high Ti/Y in the northern portion of the basin, designated Pitanga, Paranapanema, Urubici and Ribeira types; and 2) low Ti/Y predominant in the southern portion of the basin, designated Gramado and Esmeralda types.

The felsic rocks (SiO_2>62 wt.%) are mostly rhyodacites, dacites, quartz latites and subordinately rhyolites, divided into two chemical types. The high Ti, P (and La, Ce, Zr) felsic rocks are designated Chapecó type and the low Ti, P are the Palmas type (Bellieni et al., 1986).

2. Sampling strategy and analytical methods

The four rocks for this isotopic investigation were selected from many samples collected by the authors during several 2004–2008 field seasons and from the rock collection of CPRM (Geological Survey of Brazil), Porto Alegre office. Our sampling includes three stratigraphic units (Fig. 1a and b). Data on each sample (coordinates, rock name, stratigraphic unit, and number of analyses per sample) and previous Ar–Ar ages from rocks with similar compositions to the samples dated in this work are summarized in Table 1. All rocks were investigated in thin sections and had whole-rock chemical analyses performed (Table 2).

2.1. Sample description and petrography

Sample VIF is basalt collected in a quarry near BR-386 highway near the Uruguay River within Iraí town. The basalt lava is ~30 m thick and consists of a thin (~0.5 m) vesicular lower crust, massive core with columnar jointing and a highly vesicular upper crust with irregular jointing, breccias and a thin layer (0.5 m) of silicified sandstone on top. The sample is from the massive core with columnar jointing. This basalt sample was selected for zircon geochronology because it has 268 ppm Zr, so zircon probably precipitated from the melt. The fine to medium-grained texture of the rock indicates that zircon crystals may be sufficiently large for SHRIMP analysis.

Sample VIF is composed of labradorite (~65 vol.%), augite and minor pigeonite (~30%), Ti-magnetite and ilmenite (~5%), with apatite as an ubiquitous accessory mineral. The sample has a glomeroporphyritic to porphyritic texture with plagioclase and minor clinopyroxene phenocrysts. Interstitial material in the groundmass consists of variable proportions of plagioclase, clinopyroxene, quartz, K-feldspar and Fe–Ti oxides. Zircon was not observed in thin section.

Sample WWP is from the Palmas type and was collected in São Francisco de Paula town, Rio Grande do Sul state, in the Serra Geral escarpment, corresponding in part of the TS (Taquara–São Francisco) road profile, previously studied by Piccirillo et al. (1988). The flow is tabular, ~40 m thick and consists of 1–5 m of vesicular and brecciated lower crust, 25 m massive core with columnar jointing, and a 10 m vesicular upper crust marked by prominent flow banding and flow breccia. This rhyodacite is nearly aphyric to weakly porphyritic with a few sparse plagioclase and rare augite microphenocrysts (<0.2 mm). The groundmass is composed of quartz, K-feldspar, plagioclase, pyroxene, magnetite and ilmenite. The content of Zr (227 ppm) made this a favorable rock for zircon isotopic studies.

The dated sample WW254 was collected from PR-170 road near Foz do Areia hydroelectric facility, and WW255 sample was collected in a quarry in Guarapuava town. The flows are tabular ranging in thickness from 40 to 60 m, with horizontal jointing at the bottom and prominent flow banding that evolves to flow folds and flow breccias at the top. Petrographically, the rocks are porphyritic, with K-feldspar and plagioclase euhedral phenocrysts prominent in a vitrophyric matrix with crystallites of plagioclase, quartz and K-feldspar. The clinopyroxene is pigeonite and forms glomeroporphyritic aggregates. Zircon and oxyhornblende were observed in thin section as accessories only in this volcanic sub-type, with some apatite and

Table 1
Summary of age results obtained by zircon U–Th–Pb analyses of zircons (errors = 2σ) on four samples in this work; (h) = elevation above sea level; (n) = number of spots analyzed.

Sample	Magma type	Rock type	Easting[a]	Northing[a]	h (m)	Age (Ma)	±	MSWD	n
VIF	Pitanga	Basalt	0276930	6991150	230	134.4	1.1	0.48	8
WWP	Palmas	Rhyodacite	0541620	6740982	907	134.6	1.4	0.80	10
WW254	Chapecó	Quartz latite	0490251	7132871	1170	134.8	1.4	0.70	9
WW255	Chapecó	Quartz latite	0450575	7187968	1090	135.6	1.8	2.40	8

[a] Coordinates in UTM (Córrego Alegre datum).

Table 2
Major oxides (wt.%) and trace-element (ppm) abundances for Paraná volcanic rock samples dated in this work. (<DL) = below detection limit.

	VIF	WWP	WW254	WW255
SiO_2	49.75	65.02	63.60	64.04
TiO_2	3.95	0.94	1.45	1.41
Al_2O_3	12.78	13.25	12.87	13.08
Fe_2O_3	14.78	6.58	7.84	7.86
MgO	4.34	1.64	1.44	1.30
CaO	8.19	3.45	3.18	3.22
Na_2O	2.59	3.13	3.15	3.36
K_2O	1.56	3.88	4.10	3.96
P_2O_5	0.48	0.26	0.48	0.46
MnO	0.19	0.11	0.14	0.15
Cr_2O_3	0.005	<DL	<DL	<DL
LOI	1.30	1.50	1.50	0.90
Total	99.7	99.8	99.75	99.75
Ba	431	566	1041	1006
Rb	30	144	107	108
Sr	516	160	392	444
Y	37	33	69	69
Zr	268	227	590	587
Nb	23.8	21.3	52	52.7
Th	2.8	13.0	10.0	9.7
U	0.7	5.7	2.4	2.4
Hf	7.3	6.5	15.9	16.2
Ga	23	18	25	26
Sn	2.0	7.5	5.0	5.0
Cu	37	27	13	13
Ni	20.0	8.8	15.6	8.7
Be	1	3	3	2
Co	40.6	13.6	7.1	6.8
Cs	0.3	5.9	1.9	1.7
Ta	1.4	1.6	3.3	3.2
V	455	90	52	45
W	0.5	1.5	1.3	1.0
La	32	36	74	73
Ce	71	74	170	168
Pr	9.99	9.45	20.50	20.30
Nd	43.5	38.4	93.8	91.1
Sm	9.42	7.47	18.00	18.20
Eu	2.93	1.55	4.40	4.80
Gd	8.79	7.09	14.10	13.80
Tb	1.48	1.17	2.40	2.40
Dy	7.78	6.38	12.70	12.40
Ho	1.33	1.31	2.40	2.30
Er	3.58	3.89	6.40	6.40
Tm	0.53	0.56	0.90	0.90
Yb	3.01	3.55	6.00	5.60
Lu	0.46	0.52	0.80	0.80
Ti/Y	642	171	126	122

Fe–Ti oxides. Accordingly, Zr content is very high in the rocks (WW254 = 590 ppm and WW255 = 587 ppm).

3. Analytical methods

3.1. Geochemical methods

The dated rock samples were analyzed for major and trace elements at the ACME Analytical Laboratories, Vancouver, Canada. Major elements and several trace elements were determined by ICP–emission spectrometry following a Lithium metaborate/tetraborate fusion and dilute nitric digestion. Loss on ignition (LOI) was determined by weight difference after ignition at 1000 °C. Total iron is indicated as Fe_2O_3. Rare earth and refractory elements were analyzed by inductively coupled plasma mass spectrometry (ICP–MS) following the same decomposition method of major elements. Pure elemental standard solutions were used by ACME for calibration and SO-18 for major and trace elements and DS-7 for metals analyses were used as reference materials. The analytical accuracies are estimated to be 0.01% for major oxides (Appendix A). The accuracies of the ICP–MS analyses (Appendix B) are estimated to be better than ±5% (relative) for most elements (Qi and Zhou, 2008).

3.2. U–Pb SHRIMP methodology

Following the methodology of Santos et al. (2008), the rock samples were crushed, milled and sieved to <250 μm. Heavy minerals were separated using heavy liquid (TBE, tetra-bromo-ethane) and magnetic separation techniques were used to concentrate the non-magnetic zircon. Final separation of the grains was by hand picking. The grains were mounted on epoxy discs with fragments of standards, ground and polished, photomicrographed in transmitted and reflected light, and imaged (backscattered electrons) for their internal morphology, using a Jeol 6400 scanning electron microscope at the Center for Microscopy and Microanalysis at the University of Western Australia. The epoxy mounts were then cleaned and gold-coated for SHRIMP analyses. The zircon standard used was BR266 ($^{206}Pb/^{238}U$ age of 559 Ma, 903 ppm U). The isotopic composition of the minerals was determined using SHRIMP II (De Laeter and Kennedy, 1998), using methods based on Compston et al. (1992). Zircon was analyzed using a primary ion beam of ~4 nA, 10 kV O_2^{2-} with a diameter of ~25 μm, focused onto the mineral. In the Palmas sample, we used a weaker primary beam (~1.2 nA) in two analyses (a.1-4b and f.1-1) to prevent the ThO^{2+} signal from exceeding that tolerated by the ion counter. For each spot analysis, initial sputtering was used to remove the gold and surface common lead before analysis. Although the $^{207}Pb/^{206}Pb$ age is imprecise and sensitive to the common Pb correction, only four of the 50 analyses were not within 2σ analytical error of concordance. Results with more than 0.5% common ^{206}Pb correction are presented but not used in age calculations, except in sample VIF where all data were considered. Zircon data are reduced using SQUID (Ludwig, 2002). Data were plotted on weighted average and Concordia diagrams using ISOPLOT/Ex software (Ludwig, 1999); error ellipses on Concordia plots are shown at the 95% confidence level (2σ). The analytical uncertainty in all grouped age data is quoted at the 95% confidence level (2σ).

4. Results

4.1. Geochemistry

An overview of the geochemical composition of the four dated samples and of the volcanic sequence (data from Comin-Chiaramonti et al., 1988; Peate, 1990; Peate et al., 1990, 1999; Peate and Hawkesworth, 1996; Garland et al., 1995, 1996; Nardy et al., 2008) is displayed on the TAS (Fig. 2a) diagram. Sample VIF has ~50% SiO_2 and ~4% MgO, while the other samples have >63% SiO_2 and ~1.5% MgO (Table 2). Using the total alkali–silica plot of Le Bas et al. (1986), the VIF sample is classified as tholeiitic basalt, WWP as dacite, whereas WW254 and WW255 are trachydacites. However, using the chemical variation diagram of De La Roche et al. (1980), not shown in this work, the VIF sample lies within the basaltic andesite field, WWP sample can be classified as rhyodacite, whereas WW254 and WW255 lie between rhyodacite and quartz latite. The terminology of classification is not clear-cut because of different criteria, so we hereafter classify VIF sample as basalt, WWP as rhyodacite, WW254 and WW255 as quartz latite based on the CIPW norms (Cross et al., 1902).

High Ti/Y basalts of the Pitanga magma type have a close spatial association with the Paranapanema magma type (also high-Ti) in the Paraná magmatic province. Together, they comprise approximately 50% of the total preserved lava volume (Peate, 1997). The Pitanga magma type has Ti/Y higher than Paranapanema; typically Pitanga basalts have 3.5 wt.% TiO_2 whereas Pananapanema basalts have only 2.5 wt.% TiO_2 (Fig. 2b). In the studied region, the Paranapanema lavas overlie Pitanga lavas, and this is in agreement with the outcrop pattern and borehole data in other Paraná province areas, as observed by Peate et al. (1992). Although these magma types are dominant to

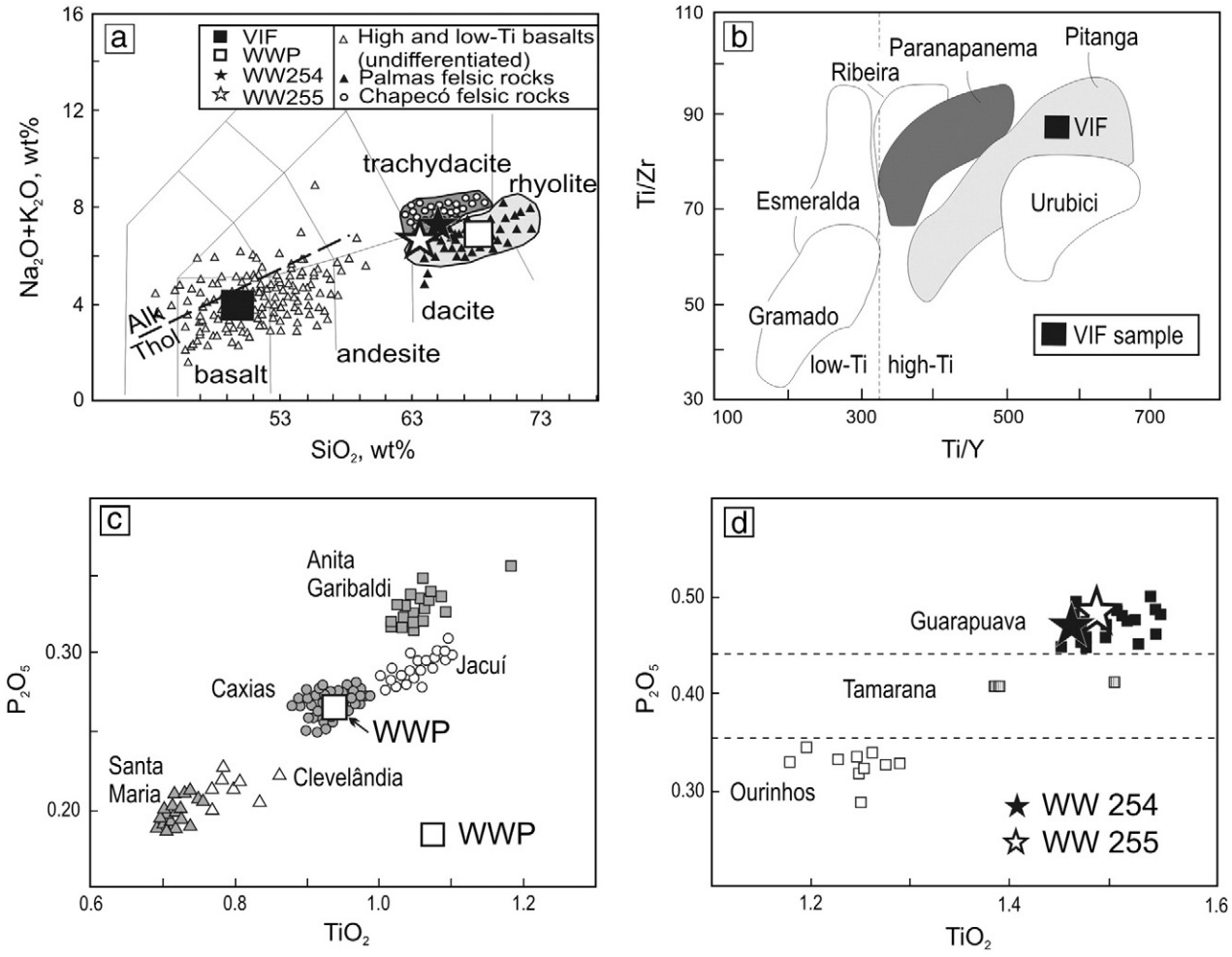

Fig. 2. (a) Classification of the Paraná magmatic province according to Le Bas et al. (1986), the compositional variation of high- and low-Ti basalts (white triangles) data from Comin-Chiaramonti et al. (1988), Peate (1990), Peate and Hawkesworth (1996) and Garland et al. (1996); shaded field encloses published analyses of Palmas (black triangles) and Chapecó (circles) felsic rocks classified according to Garland et al. (1995) and Nardy et al. (2008); (b) Ti/Y vs Ti/Zr diagram, showing the classification of VIF sample in the basaltic magma types of the Paraná magmatic province (after Peate, 1997); (c, d) TiO_2 vs P_2O_5 diagram showing the classification of WWP and WW 254 and WW 255 samples in the felsic types of the Paraná magmatic province (Nardy et al., 2008): (c) Discrimination diagram of sub-types of Palmas felsic type; (d) diagram of sub-types of Chapecó felsic type. Fields of classification enclose published data from Nardy et al. (2008). Samples dated in this investigation highlighted in all four figures.

the north of the Rio Piquiri lineament (Piccirillo et al., 1988), we sampled rocks immediately to the south of the Rio Uruguay lineament (Fig. 1a).

The dated sample WWP is from the Palmas magma type and overlies low-Ti Gramado basalts (Fig. 1b) in the Serra Geral escarpment. The Palmas type felsic rocks cover an area of 40,324 km^2 and were subdivided into two types (five subtypes) by Nardy et al. (2008) based principally on Ti and P contents: Santa Maria and Clevelândia ($TiO_2 \leq 0.87\%$); Caxias do Sul, Anita Garibaldi and Jacuí ($TiO_2 \geq 0.90\%$). The sample is from the Caxias do Sul sub-type (Fig. 2c), because it has 0.94 wt.% TiO_2 and 0.26 wt.% P_2O_5. This type was first recognized by Peate et al. (1992) and covers an area of 16,000 km^2 with a volume of 4832 km^3 (Nardy et al., 2008).

Samples WW254 and WW255 have compositions of quartz latites (Table 2): 18% normative quartz, 24–25% orthoclase, and 36–38% plagioclase (ab + an).

The dated quartz latites are from Chapecó felsic type and overlie high-Ti basalts (Fig. 1b). This type covers an area of 6617 km^2 with a maximum thickness of 270 m (Nardy et al., 2001), exposed near Faxinal do Céu and Guarapuava towns (Paraná state), and Nonoai and Chapecó towns (Rio Grande do Sul state).

A compositional variation within the high-Ti Chapecó type felsic volcanics (Piccirillo et al., 1987) led Peate et al. (1992) to subdivide it into the Ourinhos sub-type ($Rb/Zr > 0.2$, $^{87}Sr/^{86}Sr_i = 0.7076–0.7080$), exposed over a restricted area, and the widespread Guarapuava sub-type ($Rb/Zr < 0.2$, $^{87}Sr/^{86}Sr_i = 0.7055–0.7060$). Nardy et al. (2008) subdivided the Chapecó magma type into three sub-types (Ourinhos, Tamarana and Guarapuava subtypes) based in TiO_2 and P_2O_5 contents. Samples WW254 and WW255 have similar contents of TiO_2 (1.45 and 1.41 wt.%) and similar P_2O_5 (0.48 and 0.46 wt.%), and are of the Guarapuava subtype (Fig. 2d).

4.2. U–Pb geochronology

4.2.1. Zircon morphology

The analyzed zircon crystals are weakly zoned and have an otherwise homogeneous texture. Most grains are clear, weakly colored and small to medium sized (50–100 μm length), except a few zircon grains from the Chapecó porphyritic quartz latite that have grains up to 600 μm long. Only the WWP sample (Palmas rhyodacite) has quartz inclusions; the other three are inclusion-free. The exact original size and shape distribution of the zircon crystals, in general, is difficult to assess because most grains were broken, especially from the WWP sample (Palmas rhyodacite), presumably during sample preparation. But in general the VIF (Pitanga basalt) zircon population is anhedral to subhedral, similar to many zircons from kimberlite, alkali basalt (Pupin et al., 1978) and other magmas of deep-seated, mantle origin (Corfu et al., 2003).

On the other hand, in the felsic rocks the zircon crystals show distinct characteristics. The zircon crystals from rhyodacite WWP are highly irregular with rounded outlines, whereas in the porphyritic quartz latite WW254 and WW255, zircon crystals are prismatic, needle-shaped, without bipyramidal terminations, characteristic of a more rapid (quench) crystallization (Fig. 3b).

4.2.2. U–Pb SHRIMP analytical results

The SHRIMP analyses were carried out avoiding fractures and inclusions, but some grains were too fractured to avoid overlap of the analysis area onto fractures. Details of U–Pb data are presented in Table 3.

4.2.2.1. Sample VIF — Pitanga-type basalt. We separated 12 zircons crystals (Fig. 3a) from this basalt. All crystals are broken and show few crystal faces. One crystal is xenocrystic and three crystals were too small or fractured to be analyzed. For a test, we analyzed two broken crystals (analyses b.0-1 — showed in Fig. 3a and b.4-2), but these resulted in lower and higher than average ages and were discarded as outliers. Overall, we used eight of the ten zircon analyses from grains with sizes between 30 and 100 μm. Some of the crystals analyzed are shown in Fig. 3a.

The weighted mean $^{206}Pb/^{238}U$ age of the eight analyses yields 134.4 ± 1.1 Ma (MSWD = 0.48) which is interpreted as the crystallization age of this high-Ti basaltic rock (Fig. 4a). The Th/U ratios of the zircons are very high, with a range of 2.72–11.58 and an average of 5.38.

4.2.2.2. Sample WWP — Palmas rhyodacite, Caxias do Sul sub-type. The low-Ti rhyodacite had few zircon grains, with only five crystals separated from 10 kg of rock. However two grains, in spite of fractures, are large and have a mean diameter of ~100 μm (Fig. 3c and d). We analyzed the zircons in three different sessions. The grains were analyzed in the first session, and then the mount was repolished for the second session (analyses a.1 and a.2). In the third session (analysis a.3) we selected two more grains for analyses in another mount (see Table 3).

A total of 16 spot analyses were made on zircon grains from the WWP sample, but seven analyses resulted in discordant ages (either lower or higher). These six analyses were obtained from two small grains (~25 μm, analyses z.1.1 and z.1.2) and the other four analyses (a.1-4, a.1-5, a.2-5 and a.2-7) came from a fractured grain where the analysis area included fractures (Fig. 3c, d). The remaining 10 analyses yield a weighted average $^{206}Pb/^{238}U$ age of 134.6 ± 1.4 Ma (MSWD = 0.8). The Concordia ages of these zircon grains are illustrated in Fig. 4b. The Th/U ratio (unanalyzed in a.1–4b and f.1-1 because of the high Th value) has a mean ratio of ~1.5 and a range of 0.89 to 2.09 and the U contents are very high (1844 to 4829 ppm), with a mean of 3525 ppm.

The high U contents may cause a matrix effect that biases ages to be older (Williams and Hergt, 2000) but we observed no correlation between age and U content to suggest that this analytical effect influenced the age data. The three youngest ages all had U contents higher than average, and we conclude that these ages are statistical outliers related to the proximity of fractures in the analyzed grain (Fig. 3c and d).

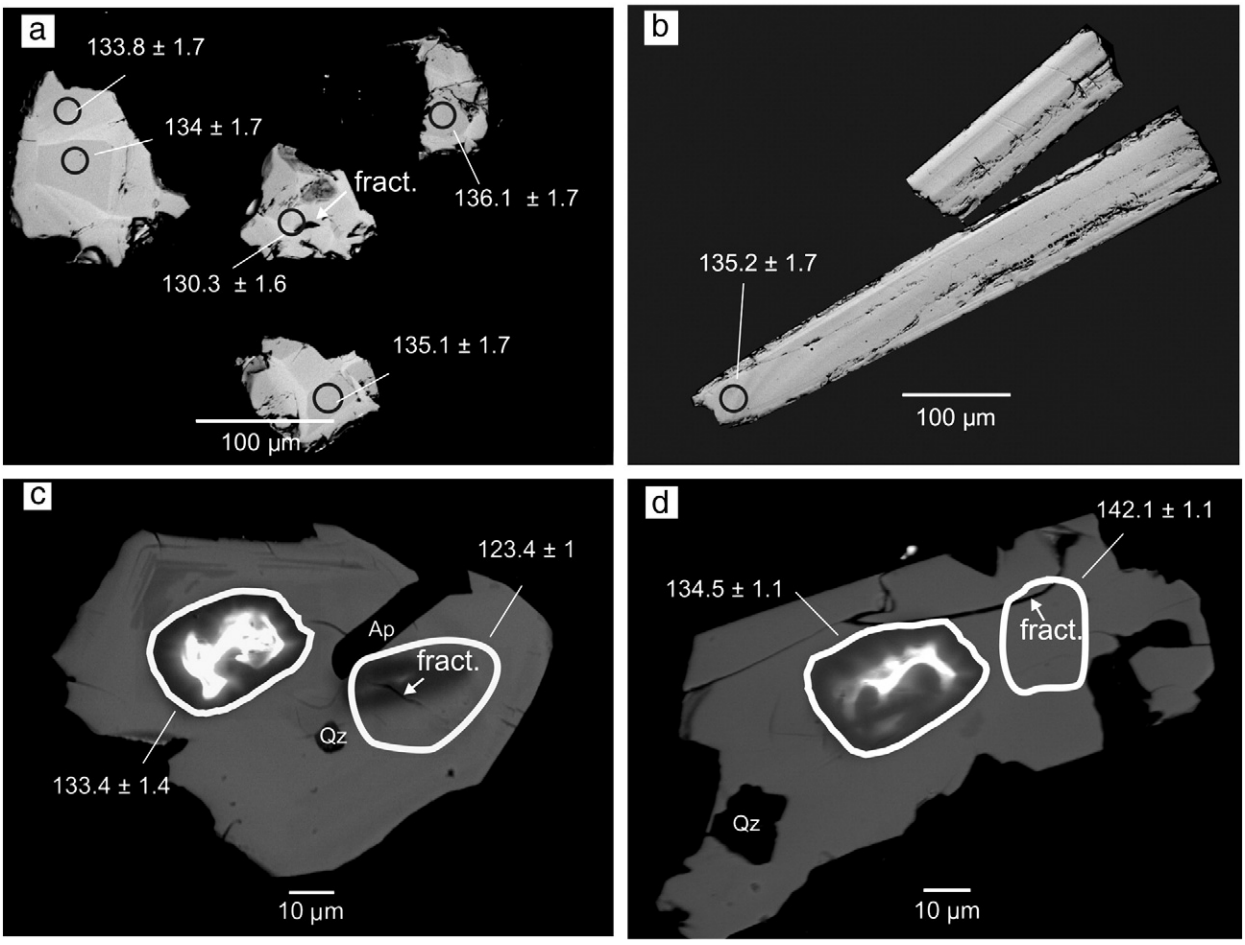

Fig. 3. BSE images of dated zircon crystals, with indication of analyzed areas and corresponding ages. Analyzed areas which include fractures are indicated and discussed in the text. (a) Basalt sample VIF, five crystals analyzed; (b) quartz latite sample WW 255; (c) and (d) rhyodacite sample WWP; Qz = quartz inclusion, Ap = apatite inclusion, fract. = fracture.

Table 3
Zircon SHRIMP U–Th–Pb isotopic data (errors = 2σ) of four volcanic rocks of the Paraná magmatic province. 4f206 (%) = (common ^{206}Pb)/(total measured ^{206}Pb) based on measured ^{204}Pb.

						Isotopic ratios				Ages	
	U	Th	Th	^{206}Pb	4f^{206}	^{238}U	^{206}Pb	^{207}Pb	^{208}Pb	^{207}Pb	^{206}Pb
Spot	ppm	ppm	U	ppm	(%)	^{206}Pb	^{238}U	^{235}U	^{232}Th	^{206}Pb	^{238}U
Basalt, sample VIF											
b.1-1	1244	4104	3.41	22	1.11	48.9625 ± 1.25	0.0204 ± 1.25	0.1309 ± 5.38	0.0063 ± 1.54	23 ± 126	130.3 ± 1.6
b.1-2	836	5106	6.31	15	0.69	46.8757 ± 1.28	0.0213 ± 1.28	0.1467 ± 3.92	0.0063 ± 1.49	190 ± 86	136.1 ± 1.7
b.1-3	860	7395	8.88	16	0.81	47.5704 ± 1.30	0.0210 ± 1.30	0.1381 ± 6.15	0.0063 ± 1.59	81 ± 143	134.1 ± 1.7
b.1-4	1025	5113	5.15	19	1.25	47.6680 ± 1.27	0.0210 ± 1.27	0.1353 ± 5.10	0.0063 ± 1.47	37 ± 118	133.8 ± 1.7
b.2-1	956	10,715	11.58	18	1.80	47.4946 ± 1.32	0.0211 ± 1.32	0.1467 ± 7.61	0.0063 ± 1.41	219 ± 173	134.3 ± 1.8
b.2-2	1167	4281	3.79	22	1.25	47.2142 ± 1.26	0.0212 ± 1.26	0.1316 ± 5.97	0.0065 ± 1.52	−53 ± 142	135.1 ± 1.7
b.3-1	1772	8983	5.24	32	0.36	47.1921 ± 1.20	0.0212 ± 1.20	0.1469 ± 3.58	0.0064 ± 1.32	207 ± 78	135.2 ± 1.6
b.3-2	1397	4442	3.29	25	0.71	48.1969 ± 1.24	0.0207 ± 1.24	0.1412 ± 5.04	0.0062 ± 1.53	165 ± 114	132.4 ± 1.6
b.4-1	1053	2769	2.72	19	1.19	47.7429 ± 1.30	0.0209 ± 1.30	0.1303 ± 7.23	0.0062 ± 1.84	−48 ± 173	133.6 ± 1.7
b.4-2	1529	5054	3.41	29	0.89	45.0734 ± 1.26	0.0222 ± 1.26	0.1385 ± 5.36	0.0065 ± 1.52	−41 ± 127	141.5 ± 1.8
Rhyodacite, sample WWP											
a.1z	3969	4708	1.23	64	0.12	53.0523 ± 1.10	0.0188 ± 1.10	0.1252 ± 1.77	0.0058 ± 1.30	108 ± 33	120.4 ± 1.3
a.1z2	4424	6589	1.54	84	0.11	45.4531 ± 1.09	0.0220 ± 1.09	0.1476 ± 1.45	0.0066 ± 1.17	132 ± 22	140.3 ± 1.5
a.1z3	2488	2155	0.89	46	0.00	46.5658 ± 1.09	0.0215 ± 1.09	0.1472 ± 1.38	0.0067 ± 1.32	181 ± 20	137.0 ± 1.5
a.2z1	2983	5422	1.88	54	0.09	47.8110 ± 1.09	0.0209 ± 1.09	0.1379 ± 1.57	0.0064 ± 1.20	90 ± 27	133.4 ± 1.4
a.2z2	4208	5610	1.38	76	0.06	47.8282 ± 1.09	0.0209 ± 1.09	0.1403 ± 1.42	0.0064 ± 1.31	131 ± 21	133.4 ± 1.4
a.2z3	4452	6758	1.57	82	0.00	46.5925 ± 1.08	0.0215 ± 1.08	0.1475 ± 1.33	0.0064 ± 1.17	188 ± 18	136.9 ± 1.5
a.2z4	4747	7115	1.55	84	0.39	48.6798 ± 1.27	0.0205 ± 1.27	0.1370 ± 1.96	0.0063 ± 1.40	117 ± 35	131.1 ± 1.7
a.1-4	3431	4136	1.25	64	0.04	45.9375 ± 0.77	0.0218 ± 0.77	0.1451 ± 1.07	0.0066 ± 0.88	116 ± 18	138.8 ± 1.1
a.1-4b	2555	n.a.	n.a	46	0.00	47.4286 ± 0.85	0.0211 ± 0.85	0.1443 ± 1.26	n.a. ± n.a.	177 ± 22	134.5 ± 1.1
a.1-5	4601	5427	1.22	88	0.04	44.8648 ± 0.76	0.0223 ± 0.76	0.1487 ± 0.96	0.0067 ± 1.20	119 ± 14	142.1 ± 1.1
a.2-5	4294	5861	1.41	79	0.11	46.5130 ± 0.76	0.0215 ± 0.76	0.1436 ± 1.14	0.0064 ± 0.91	121 ± 20	137.1 ± 1.0
a.2-6	4829	7076	1.51	89	0.05	46.5545 ± 0.76	0.0215 ± 0.76	0.1430 ± 1.13	0.0063 ± 0.86	113 ± 20	137.0 ± 1.0
a.2-7	2929	5936	2.09	49	0.09	51.7472 ± 0.78	0.0193 ± 0.78	0.1277 ± 1.15	0.0060 ± 0.89	96 ± 20	123.4 ± 1.0
a.2-8	2618	5013	1.98	43	0.00	51.7640 ± 0.79	0.0193 ± 0.79	0.1314 ± 1.55	0.0060 ± 0.98	164 ± 31	123.3 ± 1.0
a.2-9	3477	4905	1.46	64	0.10	46.8500 ± 0.77	0.0213 ± 0.77	0.1403 ± 1.23	0.0064 ± 0.90	82 ± 23	136.1 ± 1.0
f.1-1	1844	n.a,	n.a.	33	0.30	47.9362 ± 0.93	0.0209 ± 0.93	0.1373 ± 2.73	n.a. ± n.a.	86 ± 61	133.1 ± 1.2
f.1-6	2082	2959	1.47	38	0.67	47.3300 ± 1.15	0.0211 ± 1.15	0.1402 ± 2.53	0.0065 ± 1.48	105 ± 53	134.8 ± 1.5
Quartz latite, sample WW254											
d.2-1	846	2858	3.49	15	0.00	47.3647 ± 1.17	0.0211 ± 1.17	0.1479 ± 2.84	0.0066 ± 1.34	232 ± 60	134.7 ± 1.6
d.3-1	646	2140	3.42	12	0.00	48.0785 ± 1.18	0.0208 ± 1.18	0.1446 ± 2.29	0.0065 ± 2.54	215 ± 45	132.7 ± 1.6
d.4-1	1087	3265	3.10	20	0.00	46.5614 ± 1.14	0.0215 ± 1.14	0.1449 ± 2.53	0.0067 ± 1.29	144 ± 53	137.0 ± 1.6
d.7-1	856	2760	3.33	16	0.00	47.2268 ± 1.15	0.0212 ± 1.15	0.1440 ± 2.16	0.0067 ± 1.31	164 ± 43	135.1 ± 1.5
d.9-1	857	2356	2.84	15	0.00	47.7856 ± 1.16	0.0209 ± 1.16	0.1456 ± 2.25	0.0066 ± 1.35	216 ± 45	133.5 ± 1.5
d.13-1	1331	3884	3.02	25	0.03	45.6655 ± 1.12	0.0219 ± 1.12	0.1512 ± 1.71	0.0068 ± 1.23	198 ± 30	139.6 ± 1.6
d.14-1	1084	2327	2.22	20	0.00	46.4914 ± 1.14	0.0215 ± 1.14	0.1460 ± 2.16	0.0066 ± 1.31	158 ± 43	137.2 ± 1.5
d.15-1	1478	1192	0.83	27	0.00	46.2053 ± 1.13	0.0216 ± 1.13	0.1508 ± 2.22	0.0068 ± 2.20	219 ± 44	138.0 ± 1.5
d.16-1	922	3226	3.62	17	0.00	47.2467 ± 1.16	0.0212 ± 1.16	0.1417 ± 2.56	0.0067 ± 1.34	127 ± 54	135.0 ± 1.5
d.17-1	584	1723	3.05	10	0.00	47.7689 ± 1.20	0.0209 ± 1.20	0.1393 ± 2.97	0.0065 ± 1.43	111 ± 64	133.6 ± 1.6
d.19-1	1132	3141	2.87	21	0.00	46.8795 ± 1.15	0.0213 ± 1.15	0.1498 ± 3.52	0.0067 ± 1.35	238 ± 77	136.1 ± 1.6
Quartz latite, sample WW255											
c.1-1	755	2139	2.93	14	0.07	47.7788 ± 1.16	0.0209 ± 1.16	0.1448 ± 2.11	0.0065 ± 1.53	203 ± 41	133.7 ± 1.5
c.2-1	894	2721	3.15	16	0.16	48.0015 ± 1.21	0.0208 ± 1.21	0.1389 ± 2.39	0.0066 ± 1.53	116 ± 48	132.9 ± 1.6
c.5-1	1212	3345	2.85	23	0.00	45.6056 ± 1.14	0.0219 ± 1.14	0.1487 ± 3.34	0.0068 ± 1.31	157 ± 74	139.8 ± 1.6
c.7-1	1397	5294	3.92	26	0.00	46.5683 ± 1.12	0.0215 ± 1.12	0.1473 ± 1.94	0.0070 ± 1.31	183 ± 37	137.0 ± 1.5
c.9-1	1246	4261	3.53	23	0.15	46.3490 ± 1.14	0.0216 ± 1.14	0.1517 ± 2.41	0.0069 ± 1.40	241 ± 49	137.6 ± 1.6
c.10-1	1404	4363	3.21	26	0.00	45.8747 ± 1.13	0.0218 ± 1.13	0.1462 ± 1.81	0.0068 ± 1.47	131 ± 33	139.0 ± 1.6
c.11-1	1223	3227	2.73	23	0.00	46.1162 ± 1.13	0.0217 ± 1.13	0.1457 ± 1.80	0.0069 ± 1.25	135 ± 33	138.3 ± 1.5
c.12-1	1223	3227	2.73	23	0.00	46.1162 ± 1.13	0.0217 ± 1.13	0.1457 ± 1.80	0.0069 ± 1.25	135 ± 33	138.3 ± 1.5
c.13-1	1206	1897	1.63	22	0.00	46.3087 ± 1.13	0.0216 ± 1.13	0.1468 ± 1.95	0.0067 ± 1.33	162 ± 37	137.7 ± 1.5
c.15-1	1357	3820	2.91	25	0.00	45.9061 ± 1.13	0.0218 ± 1.13	0.1463 ± 2.53	0.0068 ± 1.34	133 ± 53	138.9 ± 1.6
c.17-1	834	1802	2.23	15	0.77	47.1867 ± 1.30	0.0212 ± 1.30	0.1425 ± 4.75	0.0066 ± 1.66	137 ± 107	135.2 ± 1.7
c.19-1	1141	3482	3.15	21	0.00	47.4483 ± 1.13	0.0211 ± 1.13	0.1476 ± 2.18	0.0067 ± 1.85	232 ± 43	134.4 ± 1.5

4.2.2.3. Samples WW254 and WW255 — Chapecó quartz latites, Guarapuava sub-type. The zircon crystals from WW255 sample are prismatic (100 to 600 μm long), with aspect ratio 4:1 to 10:1, and commonly without bipyramidal terminations (Fig. 3b), characteristic of rapid (quench) crystallization of volcanic rocks. The analytical results (Table 3) show high Th/U ratios, often higher than 3, and more normal U content (U > 500 ppm, mean 900–1000 ppm). Crystals from sample WW254 are similar to WW255, with crystal size ranging from 50 to 600 μm, U contents from 755 to 1404 ppm and Th/U ratio of 1.63 to 3.92.

The isotopic data from both samples yield ages of 134.8 ± 1.4 (WW254) from 9 out of 11 analytical points with a MSWD of 0.70, and 135.6 ± 1.8 Ma (WW255) from 8 out of 11 analytical points with a MSWD of 2.40 (Fig. 4c–d).

Five analyses are omitted from the above age calculations: analyses d.15-1 and d.13-1 in sample WW254 and analyses c.5-1, c.10-1 and c.15-1 in sample WW255. These all have anomalously old ^{206}Pb/^{238}U ages (> 139 Ma; Table 3), but none has > 3000 ppm U which might explain old apparent ages as due to the change in the instrumental age vs U/UO calibration curve in high-U zircons

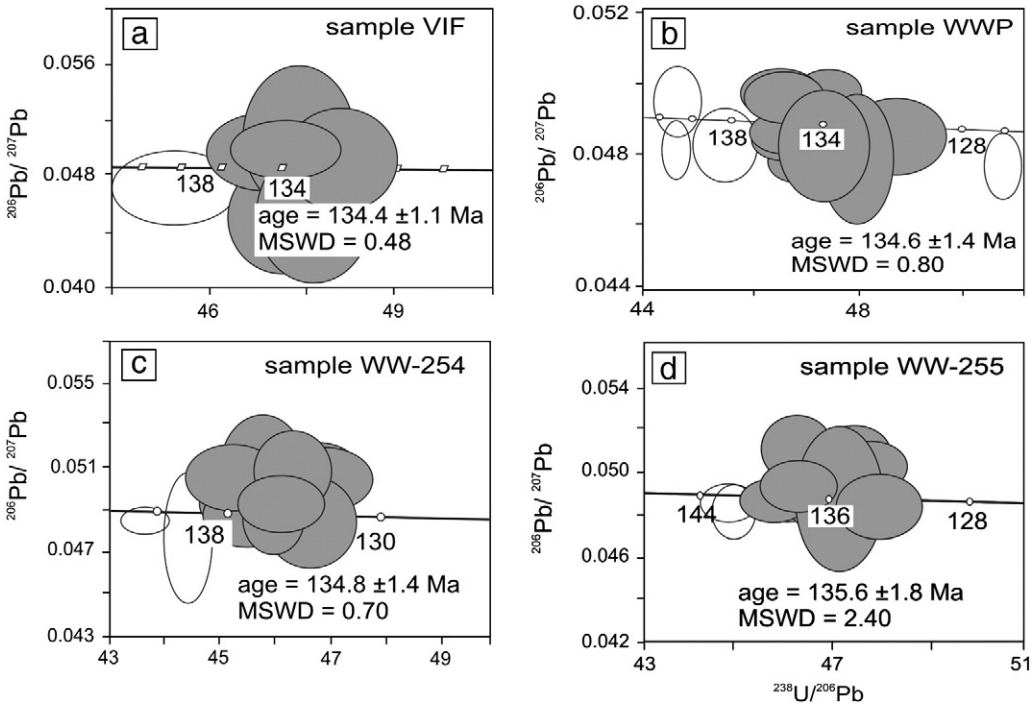

Fig. 4. Concordia of isotopic age data. (a) Pitanga basalt, sample VIF; (b) Palmas rhyodacite, sample WWP; (c) Chapecó quartz latite, sample WW254; (d) Chapecó quartz latite, sample WW255. The unfilled ellipses are from outliers not used in age calculation.

(Williams and Hergt, 2000; Aleinikoff et al., 2002). We infer these older ages as either the age of inherited xenocrysts, or overlap of the analytical area onto areas of older zircons in which case the ages are minimum ages of xenocrysts.

5. Discussion

The $^{206}Pb/^{238}U$ zircon data of this work indicate that the culmination of volcanism to the south of Rio Piquiri lineament occurred from 135.6 ± 1.8 to 134.4 ± 1.1 Ma with a maximum duration of 1–2 m.y., in the Lower Cretaceous, Valanginian–Hauterivian boundary stage. The Lower Cretaceous is probably the least well-constrained section of the geological time scale, and the age of the Valanginian–Hauterivian boundary varies by several million years between the different scales published over the last decade or so (e.g. Walker and Geissman, 2009; Gradstein et al., 2004). This is important as there have been suggestions that the Paraná–Etendeka volcanism was responsible for a carbon-isotope excursion in the Valanginian (e.g. Peate, 2009; Erba et al., 2004), but the synchronicity of the volcanism and the carbon-isotope excursion has not been robustly demonstrated yet.

In spite of numerical agreement in the ages of our four samples, they are ~2–4 m.y. older (2–3%) than the Ar–Ar ages determined by Renne et al. (1992), although their study was not on the same temporal, stratigraphic sequence of lavas. The Renne et al. (1992) study was on Gramado-type lavas from one road section on the Serra Geral escarpament on the top of the Paraná stratigraphic sequence. Some Ar–Ar ages (Turner et al., 1994; Mincato et al., 2000) obtained from rocks with similar compositions as the samples dated in this work showed ages 2–4 million years older or younger than U–Pb zircon ages. Recently Thiede and Vasconcelos (2008, 2010) used the Fish Canyon monitor to recalibrate $^{40}Ar–^{39}Ar$ and re-dated some of the same samples from the studies of Turner et al. (1994) and Stewart et al. (1996) and obtained significant different ages. The Paranapanema and Esmeralda basalts, for example, previously dated at 138.4 ± 1.3 Ma and 127.7 ± 4.6 Ma, yielded new ages of 134.0 ± 0.6 Ma and 133.5 ± 0.8 Ma, respectively (all ages relative to an age of 28.02 ± 0.09 Ma for the Fish Canyon monitor). These revisions highlight the need for careful cross-calibration of the K–Ar and U–Pb decay schemes as modern high-precision ages are increasingly identifying a mismatch between ages obtained with the different decay schemes.

There are three main models of mantle origin of Paraná magmatism: 1) Plume decompressing (e.g. Gibson et al., 1995), predicts very high eruption rates and minimal interaction with the lithospheric mantle; 2) conductive heating (e.g. Turner et al., 1996) over a protracted period of magmatism (~10 m.y.); and 3) an asthenospheric plume origin is compatible only in terms of a thermal perturbation which triggered the melting processes of the lithospheric mantle (Hawkesworth et al., 2000). The new data of the Paraná magmatism suggest that the volcanism occurred in a short period of time (1–2 m.y.). The geochemistry of the Paraná basalts is clear regarding the lithospheric mantle origin (e.g. Hawkesworth et al., 1988, 1992; Hergt et al., 1991; Marques et al., 1999), so a feasible model involves rapid heating and melting of the lithospheric mantle underlying Gondwana caused either by the rapid ascent of a plume or focussing of heat under the plate. This issue remains unresolved.

The interpretation of northward (Peate, 1997; Renne, 1997; Ernesto et al., 1999) or southeastward migration (Turner et al., 1994; Stewart et al., 1996) of Paraná volcanism cannot be resolved with the new data set, and requires additional $^{206}Pb/^{238}U$ analyses of volcanic zircons, especially in the northern part of the province (north of the Rio Piquiri lineament).

6. Conclusion

The new age data from the Paraná magmatic province from high-Ti Pitanga basalt are the best estimate for the dominant component in the early stages of the Tristan plume (Peate, 1997) and for high-Ti Chapecó quartz-latite and low-Ti Palmas rhyodacite, which are related to the late stage in continental magmatic activity. The ages are the same within the analytical error and indicate that duration of magmatism was about 1 million years, with the main pulse at ~135 Ma, in the Valanginian–Hauterivian boundary stage of the

Lower Cretaceous. More U–Pb geochronological data are required in the northern part of the province.

We have made a significant contribution to the timing of processes related to the opening of the South Atlantic Ocean and the relation between basaltic and felsic volcanic rocks in the large Paraná magmatic province.

Acknowledgements

This is a result of the PhD thesis of the first author at Universidade Federal do Rio Grande do Sul, with a "sandwich-doctorate" at the University of Western Australia. Financial support from "Conselho Nacional do Desenvolvimento Científico e Tecnológico" and "Fundação de Amparo à Pesquisa do Estado do Rio Grande do Sul" are acknowledged. Two reviewers provided considerable assistance in shaping the published version of this paper.

Appendix A. Supplementary data

Supplementary data to this article can be found online at doi:10.1016/j.chemgeo.2010.11.031.

References

Aleinikoff, J.N., Wintsch, R.P., Fanning, C.M., Dorais, M.J., 2002. U–Pb geochronology of zircon and polygenetic titanite from the Glastonbury Complex, Connecticut, USA: an integrated SEM, EMPA, TIMS, and SHRIMP study. Chemical Geology 188, 125–147.

Baksi, A.K.R., Fodor, R.V., Farrar, E., 1991. Preliminary results of $^{40}Ar/^{39}Ar$ dating studies on rocks from the Serra Geral flood basalt province and the Brazilian continental margin (abstract). Eos Trans. AGU 72 300 pp.

Bellieni, G., Comin-Chiaramonti, P.C., Marques, L.S., Melfi, A.J., Nardy, A.J.R., Papatrechas, C., Piccirillo, E.M., Roisenberg, A., 1986. Petrogenetic aspects of acid and basaltic lavas from the Parana plateau (Brazil): geological, mineralogical and petrochemical relationships. Journal of Petrology 27, 915–944.

Campos, A.C.R., Cordani, U.G., Kawashita, K., Sonoki, H.M., Sonoki, I.K., 1988. Age of the Paraná flood volcanism. In: Piccirillo, E.M., Melfi, A.J. (Eds.), The Mesozoic Flood Volcanism of the Paraná Basin: Petrogenetic and Geophysical Aspects. IAG-USP, pp. 25–46.

Coltice, N., Phillips, B.R., Bertrand, N., Ricard, Y., Rey, P., 2007. Global warming of the mantle at the origin of flood basalts over supercontinents. Geology 35, 391–394.

Comin-Chiaramonti, P., Cundari, A., Piccirillo, E.M., Gomes, C.B., Castorina, F., Censi, P., De Min, A., Marzoli, A., Speziale, S., Velazquez, V.F., 1997. Potassic and sodic igneous rocks from Eastern Paraguay: their origin from the lithospheric mantle and genetic relationships with associated Paraná Flood tholeiites. Journal of Petrology 38 (4), 495–528.

Comin-Chiaramonti, P., Bellieni, G., Piccirillo, E.M., Melfi, A.J., 1988. Classification and petrography of continental stratoid volcanics and related intrusives from the Paraná Basin (Brazil). Continental flood volcanism from the Paraná basin (Brazil). In: MacDoughall, J.D. (Ed.), Continental flood basalts. Kluwer Acad. Publ, pp. 47–72.

Compston, W., Williams, I.S., Kirschvink, J.L., Zichao, Z., Guogan, M., 1992. Zircon ages for the Early Cambrian timescale. Journal of Geological Society, London, UK 149, 171–184.

Cordani, U.G., Sartori, P.L., Kawashita, K., 1980. Geoquímica dos isótopos de estrôncio e a evolução da atividade vulcânica na Bacia do Paraná (Sul do Brasil) durante o Cretáceo. Anais da Academia Brasileira de Ciências 52, 811–818.

Corfu, F., Hanchar, J.M., Hoskin, P.W.O., Kinny, P., 2003. Atlas of zircon textures. In: Hanchar, J.M.H., Hoskin, P.W.O. (Eds.), Zircon: Reviews in Mineralogy and Geochemistry, pp. 469–500.

Cross, W., Iddings, J.P., Pirsson, L.V., Washington, H.S., 1902. A quantitative chemicomineralogical classification and nomenclature of igneous rocks. Journal of Geology 10, 555–690.

De Laeter, J.R., Kennedy, A.K., 1998. A double focusing mass spectrometer for geochronology. International Journal of Mass Spectrometry 178, 43–50.

Deckart, K., Féraud, G., Marques, L.S., Bertrand, H., 1998. New time constraints on dyke swarms related to the Paraná–Etendeka magmatism province, and subsequent South Atlantic opening, southeastern Brazil. Journal of Volcanology and Geothermal Research 80, 67–83.

De La Roche, H., Leterrier, J., Grandclaude, P., Marchal, M., 1980. A classification of volcanic and plutonic rocks using R1R2-diagram and major elements analyses — its relationships with current nomenclature. Chemical Geology 29, 183–210.

Erba, E., Bartolini, A., Larson, R.L., 2004. Valanginian Weissert oceanic anoxic event. Geology 32, 149–152.

Ernesto, M., Raposo, M.I.B., Marques, L.S., Renne, P.R., Diogo, L.A., De Min, A., 1999. Paleomagnetism, geochemistry and $^{40}Ar/^{39}Ar$ dating of the north-eastern Paraná Magmatic Province. Tectonic implications. Journal of Geodynamics 28, 321–340.

Garland, F.E., Turner, S.P., Hawkesworth, C.J., 1996. Shifts in the source of Paraná basalts through time. Lithos 37, 223–243.

Garland, F.E., Hawkesworth, C.J., Mantovani, M.S.M., 1995. Description and petrogenesis of the Paraná rhyolites. Journal of Petrology 36, 1193–1227.

Gibson, S.A., Thompson, R.N., Dickin, A.P., Leonardos, O.H., 1995. High-Ti and low-Ti mafic potassic magmas: key to plume–lithosphere interactions and continental flood-basalt genesis. Earth and Planetary Science Letters 136, 149–165.

Gradstein, F.M., Ogg, J.G., Smith, A.G., Agterberg, F.P., Bleeker, W., Cooper, R.A., Davydov, V., Gibbard, P., Hinnov, L., House, M.R., Lourens, L., Luterbacher, H.-P., McArthur, J., Melchin, M.J., Robb, L.J., Shergold, J., Villeneuve, M., Wardlaw, B.R., Ali, J., Brinkhuis, H., Hilgen, F.J., Hooker, J., Howarth, R.J., Knoll, A.H., Laskar, J., Monechi, S., Plumb, K.A., Powell, J., Raffi, I., Rfhl, U., Sanfilippo, A., Schmitz, B., Shackleton, N.J., Shields, G.A., Strauss, H., Van Dam, J., van Kolfschoten, T., Veizer, J., Wilson, D., 2004. A Geologic Time Scale 2004. Columbia University Press, Campbridge, 384 pp.

Hartmann, L.A., Wildner, W., Duarte, L.C., Duarte, S.K., Pertille, J., Arena, K.R., Martins, L.C., Dias, N.L., 2010. Geochemical and scintillometric characterization and correlation of amethyst geode-bearing Paraná lavas from the Quaraí and Los Catalanes districts, Brazil and Uruguay. Geological Magazine 147, 954–970.

Hawkesworth, C.J., Gallagher, K., Kirstein, L., Mantovani, M.S.M., Peate, D.W., Turner, S., 2000. Tectonic controls on magmatism associated with continental break-up: an example from the Paraná–Etendeka Province. Earth and Planetary Science Letters 179, 335–349.

Hawkesworth, C.J., Gallagher, K., Kelley, S., Mantovani, M.S.M., Peate, D.W., Regelous, M., Rogers, N.W., 1992. Paraná magmatism and the opening of the opening of the South Atlantic. In: Storey, B., Alabaster, A., Pankhurst, R. (Eds.), Magmatism and the Causes of Continental Break-up. : Special Publ., 68. The Geological Society, London, pp. 221–240.

Hawkesworth, C.J., Mantovani, M.S.M., Peate, D.W., 1988. Lithosphere remobilization during Paraná CFB magmatism. In: Menzies, M.A., Cox, K. (Eds.), Oceanic and Continental Lithosphere: Similarities and Differences: Journal of Petrology, pp. 205–223. Oxford.

Hergt, J.M., Peate, D.W., Hawkesworth, C.J., 1991. The petrogenesis of Mesozoic Gondwana low-Ti flood basalts. Earth and Planetary Science Letters 105, 134–148.

Kirstein, L.A., Kelley, S., Hawkesworth, C., Turner, S., Mantovani, M., Wijbrans, J., 2001. Protracted felsic magmatic activity associated with opening of the South Atlantic. Journal of the Geological Society, London 158, 583–592.

Le Bas, M.J., Le Maitre, R.W., Streckeisen, A., Zanettin, B., 1986. A chemical classification of volcanic rocks on the total alkali–silica diagram. Journal of Petrology 27 (3), 745–750.

Ludwig, K.R., 1999. Using ISOPLOT/Ex, version 2: a geochronological toolkit for Microsoft Excel. Berkeley Geochronological Center Special Publication Ia, Berkeley, California, USA. 47 pp.

Ludwig, K.R., 2002. Squid 1.02, a user's manual. Berkeley Geochronological Center Special Publication, 2. Berkeley, California, USA, 21 pp.

Lustrino, M., Melluso, L., Brotzu, P., Gomes, C.B., Morbidelli, L., Muzio, R., Ruberti, E., Tassinari, C.C.G., 2005. Petrogenesis of the early Cretaceous Valle Chico igneous complex (SE Uruguay): relationships with Paraná–Etendeka magmatism. Lithos 82, 407–434.

Mantovani, M.S.M., Marques, L.S., De Souza, M.A., Civetta, L., Atalla, L., Innocenti, F., 1985. Trace element and strontium isotope constraints on the origin and evolution of Paraná continental flood basalts of Santa Catarina State (Southern Brazil). Journal of Petrology 26, 187–209.

Marques, L.S., Dupré, B., Piccirillo, E.M., 1999. Mantle source composition of the Paraná magmatic province (southern Brazil): evidence from trace element and Sr–Nd–Pb isotope geochemistry. Journal of Geodynamics 28, 439–458.

Marsh, J.S., Ewart, A., Milner, S.C., Duncan, A.R., Miller, R. McG, 2001. The Etendeka Igneous Province: magma types and their stratigraphic distribution with implications for the evolution of the Paraná–Etendeka flood basalt province. Bulletin of Volcanology 62, 464–486.

Mincato, R.L., Schrank, A., Enzweiler, J., 2000. Geoquímica dos elementos do grupo da platina nos basaltos do norte da Província Ígnea Continental do Paraná. VIII Cong. Bras. Geoq. — Paraná, Anais, CD, cód. RE173 (PR).

Milner, S.C., Duncan, A.R., Whittingham, A.M., Ewart, A., 1995. Trans-Atlantic correlation of eruptive sequences and individual silicic units within the Paraná–Etendeka igneous province. Journal of Volcanology and Geothermal Research 69, 137–157.

Morgan, W.J., 1971. Convection plumes in the lower mantle. Nature 230, 42–43.

Nardy, A.J.R., Machado, F.B., Oliveira, M.A.F., 2008. As rochas vulcânicas mesozóicas ácidas da Bacia do Paraná: litoestratigrafia e considerações geoquímico-estratigráficas. Revista Brasileira de Geociências 38 (1), 178–195.

Nardy, A.J.R., Machado, F.B., Oliveira, M.A.F., 2001. Litoestratigrafia da Formação Serra Geral. Simpósio de Geologia do Sudeste, 7. SBG, Rio de Janeiro, p. 77.

Peate, D.W., 2009. Global dispersal of Pb by large-volume silicic eruptions in the Paraná–Etendeka large igneous province. Geology 37, 1071–1074.

Peate, D.W., Hawkesworth, C.J., Mantovani, M.S.M., Rogers, N.W., Turner, S.P., 1999. Petrogenesis and stratigraphy of the high-Ti/Y Urubici magma type in the Paraná flood basalt province and implications for the nature of 'Dupal'-type mantle in the south Atlantic region. Journal of Petrology 40, 451–473.

Peate, D.W., 1997. The Paraná–Etendeka province. In: Mahoney, J.J., Coffin, M.R. (Eds.), Large Igneous Provinces: Continental, Oceanic, and Planetary Flood Volcanism: Geophysical Monograph, 100, pp. 217–245. Washington DC, USA.

Peate, D.W., Hawkesworth, C.J., 1996. Lithospheric to asthenospheric transition in low-Ti flood basalts from southern Paraná, Brazil. Chemical Geology 127, 1–24.

Peate, D.W., Hawkesworth, C.J., Mantovani, M.S.M., 1992. Chemical stratigraphy of the Paraná lavas (South America): classification of magma types and their spatial distribution. Bulletin of Volcanology 55, 119–139.

Peate, D.W., 1990. Stratigraphy and petrogenesis of the Paraná continental flood basalts, southern Brazil, Ph.D. thesis, The Open University, Milton Keynes.

Peate, D.W., Hawkesworth, C.J., Mantovani, M.S.M., Shukovsky, W., 1990. Mantle plumes and flood basalt stratigraphy in the Paraná, South America. Geology 18, 1223–1226.

Piccirillo, E.M., Melfi, A.J., Comin-Chiaramonti, P., Bellieni, G., Ernesto, M., Marques, L.S., Nardy, A.J.R., Pacca, I.G., Roisenberg, A., Stolfa, D., 1988. Continental flood volcanism from the Paraná basin (Brazil). In: MacDoughall, J.D. (Ed.), Continental Flood Basalts. Kluwer Acad. Publ., pp. 195–238.

Piccirillo, E.M., Raposo, M.I.B., Melfi, A.J., Comin-Chiaramonti, P., Bellieni, G., Cordani, U.G., Kawashita, K., 1987. Bimodal fissural volcanic suites from the Paraná basin (Brazil): K–Ar ages, Sr-isotopes and geochemistry. Geochimica Brasiliensis 53–69.

Pupin, J.P., Bonin, B., Tessier, M., Turco, G., 1978. Rôle de l'eau sur les caractères morphologiques et la cristallisation du zircon dans les granitoides. Bulletin de la Société Géologique de France 20, 721–725.

Qi, L., Zhou, M.F., 2008. Platinum-group elemental and Sr–Nd–Os isotopic geochemistry of Permian Emeishan flood basalts in Guizhou Province, SW China. Chemical Geology 248, 83–103.

Renne, P.R., 1997. Geochronology of the Paraná–Etendeka Igneous Province. South-America Symposium on Isotope Geology — Brazil, Campos do Jordão (extended abstract) (s.n.), pp. 20–23.

Renne, P.R., Deckart, K., Ernesto, M., Ferraud, G., Piccirillo, E.M., 1996a. Age of the Ponta Grossa dike swarm (Brazil) and implications to Parana flood volcanism. Earth and Planetary Science Letters 144, 199–212.

Renne, P.R., Glen, J.M., Milner, S.C., Duncan, A.R., 1996b. Age of Etendeka flood volcanism and associated intrusions in southwestern Africa. Geology 24, 659–662.

Renne, P.R., Ernesto, M., Pacca, I.G., Coe, R.S., Glen, J., Prevot, M., Perrin, M., 1992. The age of Paraná flood volcanism, rifting of Gondwanaland, and the Jurassic–Cretaceous boundary. Science 258, 975–979.

Richards, M.A., Duncan, R.A., Courtillot, V.E., 1989. Flood basalts and hot-spot tracks: plume heads and tails. Science 246, 103–107.

Santos, J.O.S., Rizzotto, G.J., Potter, P.E., McNaughton, N.J., Matos, R.S., Hartmann, L.A., Chemale Jr., F., Quadros, M.E.S., 2008. Age and autochtonous evolution of the Sunsás Orogen in West Amazon Craton based on mapping a U–Pb geochronology. Precambrian Research 165 (3–4), 120–152.

Self, S., Thordarson, T., Keszthelyi, L., 1997. Emplacement of continental flood basalt flows. Geophysical Monograph Series, 100. American Geophysical Union, Washington, D.C, pp. 1–4.

Stewart, K., Turner, S., Kelley, S., Hawkesworth, C.J., Kirstein, L., Mantovani, M.S.M., 1996. ^{40}Ar–^{39}Ar geochronology in the Paraná continental flood basalt province. Earth and Planetary Science Letters 143, 95–109.

Thiede, D.S., Vasconcelos, P.M., 2010. Paraná flood basalts: rapid extrusion hypothesis confirmed by new ^{40}Ar–^{39}Ar results. Geology 38, 747–750.

Thiede, D.S., Vasconcelos, P.M., 2008. Paraná flood basalts: rapid extrusion hypothesis supported by new ^{40}Ar–^{39}Ar results. 44 Congresso Brasileiro de Geologia. Anais: Curitiba, PR, Brazil, Sociedade Brasileira de Geologia, p. 533.

Turner, S.P., Hawkesworth, C.J., Gallagher, K., Stewart, K., Peate, D.W., Mantovani, M.S.M., 1996. Mantle plumes, flood basalts, and thermal models for melt generation beneath continents: assessment of a conductive heating model and application to the Paraná. Journal of Geophysical Research 101, 11,503–11,518.

Turner, S.P., Hawkesworth, C.J., 1995. The nature of the subcontinental mantle: constraints from the major element composition of continental flood basalts. Chemical Geology 120, 295–314.

Turner, S.P., Regelous, M., Kelley, S., Hawkesworth, C.J., Mantovani, M.S.M., 1994. Magmatism and continental break-up in the South Atlantic: high precision ^{40}Ar–^{39}Ar geochronology. Earth and Planetary Science Letters 121, 333–348.

Walker, J.D., Geissman, J.W. 2009. Geological Time Scale 2009: Geological Society of America.

White, R.S., McKenzie, D.P., 1995. Mantle plumes and flood basalts. Journal of Geophysical Reasearch 100, 17,543–17,585.

White, R.S., McKenzie, D.P., 1989. Magmatism at rift zones: the generation of volcanic continental margins and flood basalts. Journal of Geophysical Research 94, 7685–7730.

Wildner, W., Santos, J.O.S., Hartmann, L.A., McNaughton, N.J., 2006. Clímax final do vulcanismo Serra Geral em 135 Ma: primeiras idades U–Pb em Zircão. Anais do 43° Congresso Brasileiro de Geologia, núcleo Bahia-Sergipe, Extended abstract, Aracaju-SE, Brazil, pp. 126–131.

Williams, I.S., Hergt, J.M., 2000. U–Pb dating of Tasmanian dolerites: a cautionary tale of SHRIMP analysis of high-U zircon. New Frontiers in Isotope Geoscience, pp. 185–188.